Therapeutic Targeting of Tumor-Associated Macrophages in Pancreatic Neuroendocrine Tumors

Sebastian Krug[1] ,Rami Abbassi[2], Heidi Griesmann[1], Bence Sipos[3], Dominik Wiese[4], Peter Rexin[5] Annika Blank[6], Aurel Perren[6], Johannes Haybaeck[7], Stefan Hüttelmaier[8], Anja Rinke[2], Thomas M. Gress[2] and Patrick Michl[1]

[1]Department of Internal Medicine I, Martin Luther University Halle-Wittenberg, Halle/Saale, Germany
[2]Department of Gastroenterology and Endocrinology, Philipps-University, Marburg, Germany
[3]Institute of Pathology and Neuropathology, University Hospital of Tübingen, Germany
[4]Department of Visceral, Thoracic and Vascular Surgery, Philipps-University, Marburg, Germany
[5]Institute of Pathology, Philipps-University, Marburg, Germany
[6]Institute of Pathology, University of Bern, Bern, Switzerland
[7]Institute of Pathology, Otto-von-Guericke-University, Magdeburg, Germany
[8]Institute of Molecular Medicine, Martin Luther University Halle-Wittenberg, Halle/Saale, Germany

Short title: TAMs mediate tumor progression in PNET

Key Words: TAMs, PNET, RIP1Tag2, angiogenesis

Figures: 4
Tables: 3
Suppl. Figures: 3
Suppl. Tables: 1

Novelty and Impact

The pivotal role of TAMs in PNETs has not been elucidated yet. Based on the assessment of TAM infiltration in more than 100 human specimens of metastatic and non-metastatic, functional active and non-functional active PNETs, we characterized their impact on tumor progression. Moreover, TAMs are associated with increased proliferation and angiogenesis in the RIP1Tag2 neuroendocrine mouse model. Targeting TAMs in this mouse model with the liposomal bisphosphonate clodronate led to a significant disruption of tumor progression. These findings indicate that TAMs play a major role in mediating acquired resistance to targeted antiangiogenic therapies and represent a novel therapeutic avenue to target tumor progression and drug resistance in PNETs.

Corresponding Author
Prof. Dr. Patrick Michl
Martin Luther University Halle-Wittenberg
Department of Internal Medicine I
Ernst-Grube-Str. 40, 06120 Halle (Saale), Germany,
Email: patrick.michl@uk-halle.de
Tel: 0049 345 557 2661
Fax: 0049 345 557 2253

ABSTRACT

Pancreatic neuroendocrine tumors (PNETs) represent a heterogeneous group of neuroendocrine neoplasms with varying biological behaviour and response to treatment. Although targeted therapies have been shown to improve the survival for patients at advanced stage, resistance to current therapies frequently occurs during the course of therapy. Previous reports indicate that the infiltration of tumor-associated macrophages (TAMs) in PNETs might correlate with tumor progression and metastasis formation. We aimed to evaluate the prognostic and functional impact of TAMs in human PNETs *in vitro* and *in vivo* and to investigate the effect of therapeutic targeting TAMs in a genetic PNET mouse model. TAM expression pattern was assessed immunohistochemically in human PNET tissue sections and a tissue-micro-array of PNET tumors with different functionality, stage and grading. The effect of liposomal clodronate on TAM cell viability was analysed in myeloid cell lines and isolated murine bone macrophages (mBMM). *In vivo*, RIP1Tag2 mice developing insulinomas were treated with liposomal clodronate or PBS-Liposomes. Tumor progression, angiogenesis and immune cell infiltration were assessed by immunohistochemistry.

In human insulinomas TAM density was correlated with invasiveness and malignant behaviour. Moreover, TAM infiltration in liver metastases was significantly increased compared to primary tumors. *In vitro*, liposomal clodronate selectively inhibited the viability of myeloid cells and murine bone macrophages, leaving PNET tumor cell lines largely unaffected. *In vivo*, repeated application of liposomal clodronate to RIP1Tag2 mice significantly diminished the malignant transformation of insulinomas, which was accompanied by a reduced infiltration of F4/80 positive TAM cells and simultaneously by a decreased microvessel density, suggesting a pronounced effect of clodronate-induced myeloid depletion on tumor angiogenesis. Concomitant treatment with the antiangiogenic TKI sunitinib, however, did not show any synergistic effects with liposomal clodronate. TAMs are crucial for malignant transformation in human PNET in particular in insulinomas and correlate with metastatic behaviour. Pharmacological targeting of TAMs via liposomal clodronate disrupts tumor progression in the RIP1Tag2 neuroendocrine tumor model and was associated with reduced tumor angiogenesis Based on these results, using liposomal clodronate to target proangiogenic myeloid cells could be employed as novel therapeutic avenue in highly angiogenic tumors such as PNET.

INTRODUCTION

During the last decade, the predominant role of the tumor microenvironment (TME) as modulator of tumor progression has been increasingly recognized. Non-malignant stromal cells may not only facilitate tumor initiation, disease progression and metastasis, but are also affecting response or resistance to various therapeutic strategies. The TME comprises stromal cells such as endothelial cells, fibroblasts as well as various immune cell populations [1]. Both lymphoid and myeloid lineages are modulating tumorigenesis and tumor progression, with impact on tumor cell proliferation, invasion and survival as well as effects on the immunogenicity of the tumor [2, 3]. Within the myeloid compartment, tumor-associated macrophages (TAMs) represent an important fraction. Numerous studies have demonstrated an inverse correlation between patient prognosis and TAM infiltration in various tumor entities, among them Hodgkin's lymphoma, breast cancer, glioblastoma and pancreatic cancer [4-7]. The functional impact of TAMs is still incompletely understood. TAMs release miscellaneous cytokines and proteases, among them pro-angiogenic factors such as VEGF as well as various cathepsins [8-10]. In addition to their profound effects on tumor progression, TAMs equally affect the efficacy of cancer therapy and the effects of therapeutic irradiation and targeted antiangiogenic treatment are modulated by TAMs which may acquire different functional states during tumor initiation, progression and therapeutic intervention. TAM functional plasticity has been categorized in two different opposing polarization states, M1 and M2. Generally, M1 macrophages secrete pro-inflammatory cytokines with anti-neoplastic effects while M2 macrophages produce anti-inflammatory signals which facilitate tumor progression [11, 12]. However, it is noteworthy that this classification is oversimplified and does not fully represent the complexity of TAM action.

Pancreatic neuroendocrine tumors (PNETs) represent a heterogeneous tumor entity within the group of neuroendocrine neoplasms. From a clinical point of view, patients with functionally active PNETs (FA-PNETs) such as insulinomas are mainly diagnosed at early stages, whereas non-functional PNETs (NF-PNETs) often present with symptoms when distant metastases have already occurred [13]. Several clinicopathological features have been linked to poor overall survival, including performance status, age, differentiation and proliferation capacity (Ki-67 index) [14-16]. In recent years, effort has been made in deciphering the genetic basis of PNETs.

Commonly mutated genes include MEN1, DAXX, ATRX and members of the mTOR pathway [17]. Recently, whole-genome sequencing results of more than 100 PNETs were presented by Scarpa and co-workers. In this landmark paper novel germline mutations in the genes MUTYH, CHEK2 and BRCA2 were described [18]. Moreover, distinct subgroups with altered somatic mutations were identified, including chromatin remodelling, DNA damage repair, activation of mTOR signalling (DEPDC5 and EWSR1) and telomere modification [18].

The influence of infiltrating immune cells in neuroendocrine tumors has not been completely elucidated yet. In humans, infiltration of TAMs in primary PNETs correlates with proliferative activity, presence of liver metastases and disease recurrence after curative surgery [19, 20]. Preclinical studies to decipher the role of immune cells were performed using the RIP1Tag2 genetically engineered mouse model for pancreatic neuroendocrine tumors. This model faithfully recapitulates the multistep process of insulinoma transformation, including the stages of hyperplastic islets, angiogenic islets, and invasive tumors with various gradings [21]. When tissue bound macrophages were constitutively depleted in RIP1Tag2 mice via genetic CSF-1 deficiency the tumor burden decreased markedly [19].

Mechanistically, TAMs modulate the tumor micromilieu via secreting multiple mediators of angiogenesis and invasiveness such as VEGF, heparanase and cathepsins [9, 22-24]. To overcome TAM mediated disease progression, clinically feasible therapeutics are mandatory. To this end, we utilized liposomal clodronate as pharmacological tool to target TAMs in the RIP1Tag2 model. Moreover, in two large series of FA- and NF-PNETs and in primary and distant metastatic sites CD68 positive macrophages were assessed to study the association between TAM infiltration and tumor progression in humans.

MATERIALS AND METHODS

Material and Cell Lines

Human neuroendocrine Bon-1 and QGP1 cells were a kind gift of R. Göke, University of Marburg, Germany ([25], passage 10-30) and cultured in DMEM/HAM's F12 medium. J774 and RAW cells were obtained by ATCC and cultured in Dulbecco's modified Eagle's medium (GIBCO) supplemented with 10% FCS. All media contained 10% fetal bovine serum and 40 µg/ml gentamicin. All cells were cultured in a humidified atmosphere containing 5% CO_2 at 37°C.

Immunohistochemistry, construction of tissue arrays and evaluation

Ki-67 proliferation index was evaluated according to a standardized protocol using Leica-Bond-Max-Autostainer and the Ki-67 antibody from Dako at a dilution of 1:1000. In addition, CD31 (1:20; Dianova; Hamburg, Germany) and CD68 (Dako, 1:100) antibodies were used. Antibody binding was visualized using a biotinylated secondary antibody, avidin-conjugated peroxidase (ABC method; Vector Laboratories), 3,39 diaminobenzidine tetrachloride (DAB) as a substrate, and H&E as counterstain.

Immunohistochemical staining for CD3 (1:500; abcam), F4/80 (1:50; abDSerotec, BioRad), Caspase-3 (1:100; Cell Signaling), SV40-T-antigen V-300 (1:100; Cell Signaling), FOXP3 (1:50; Affymetrix) and Arginase I (1:50; Santa Cruz) was performed using Leica-Bond-RX. Visualization was performed using Bond Polymer Refine Detection and H&E as counterstaining.

The insulinoma tissue samples (FFPE) were obtained from the neuroendocrine tumor archives of the Departments of Pathology in Zürich (Switzerland), Düsseldorf (Germany) and Kiel (Germany) from 1975 – 2006 according to the guidelines of the local ethics committees. 1.5-mm tissue cores were taken from representative areas and inserted into four paraffin blocks. The 4 MTAs contained a total of 286 cores and additional human tonsil orientation/control cores. The construction was performed using MTA1 tissue arrayer equipment (Beecher Instruments, Sun Prairie, WI, USA). MTAs were routinely processed for paraffin sectioning. Paraffin sections were deparaffinized, rehydrated and immunohistochemical stains were performed according to routine methods. The analysis was performed by a pathologist with expertise in endocrine and pancreatic tumors (B.S.) in a blinded fashion concerning clinical tumor parameters.

Transgenic mouse model and treatments

The RIP1Tag2 transgenic mouse model has been previously described [21, 26, 27]. RIP1Tag2 mice were generated and maintained in a C57BL/6 background. No glucose-enriched food or water was offered to diminish the risk of hypoglycemia. Liposomal clodronate and PBS-Liposomes were obtained from Dr N Van Rooijen (Vrije Universiteit, Amsterdam, Netherlands). Liposomal clodronate was injected intraperitoneally twice per week at concentrations of 1.4mg/20mg body weight.

Sunitinib malate was purchased from Cayman chemical (Ann Arbor, USA) and administered daily by oral gavage at concentrations of 40 mg/kg/d. All animal experiments were approved by the local government authorities and performed according to the guidelines of the animal welfare committee.

Statistical design and analysis

The comparisons between macrophage infiltration, tumor response and histopathological characteristics, disease stage and laboratory features were performed based on Chi-square and Fisher's exact tests, as appropriate. Recurrence-free survival was measured from surgery to recurrence, disease-related death, or last follow-up. OS was measured from the beginning of treatment to the time of last follow-up or death. Actuarial survival was measured by the method of Kaplan and Meier [28]. All data are presented as mean ± standard error deviation. Two-tailed paired Student's t test was used for statistical evaluation of the data. The one-way and non-parametric ANOVA test was used to calculate the p value for more than two groups. A p value < 0.05 was considered significant. All statistical calculations were performed using SPSS (IBM SPSS Statistics) and graph pad prism (GraphPad software, La Jolla, USA).

RESULTS

Impact of TAMs in functional- (FA) and functional non-active (NF) PNETs

TAM infiltration was initially assessed in a cohort of PNET tissues including 21 insulinomas as well as 11 non-metastatic NF tumors and 13 metastatic NF tumors (Figure 1A). Baseline characteristics of all patients within this cohort are given in Table 1. As expected due to earlier presentation with symptoms, insulinoma patients were younger than NF-PNET patients, which was independent of the presence or absence of distant metastases (median age: 48 vs. 54 vs. 58 years, table 1). Likewise, higher grading significantly correlated with metastatic behaviour (G1 1 metastatic vs. 9 non-metastatic, G2 12 metastatic vs. 2 non-metastatic tumors; P=0.006), confirming the influence of proliferation on disease progression. In this cohort, CD68 positive macrophages were counted in at least 10 HPF. Representative immunohistochemical stainings are shown in Figure 1B. Mean TAM infiltration in primary tumors did not differ between insulinomas, metastatic NF-PNET and non-metastatic NF-PNET (163, 170 and 133 CD68+ cells / 10 HPF, respectively) (Fig.

1C). In contrast, TAM infiltration in metastases (430 CD68+ cells / 10 HPF) was markedly higher compared to primary tumor tissues, with significance being reached in comparison to insulinomas and non-metastatic NF-PNETs (P=0.004 and P=0.021) (Fig. 1C). Comparison of the FNA-PNET metastases to primary FNA-PNET tumor tissues (only 1 paired and 3 independent primary tumor samples) did not reach significance due to a small number of samples of available primary FNA-PNET tissues (P=0.082) (Fig. 1C). None of the patients with metastatic disease received anti-resorptive therapy with bisphosphonates.

In subgroup analyses, no correlation between TAM infiltration and patient age, tumor grading, Ki-67 or recurrence-free survival was detected, most likely due to small and heterogeneous sample sizes. Thus, we decided to assess TAM infiltration in an independent larger cohort. For this purpose, a multiple-tissue-array (MTA) was used comprising 83 tissue with benign and malignant insulinomas and normal peritumoral exocrine pancreatic tissues as internal controls. Histopathological characteristics of the patients are presented in supplementary table 1. Twelve patients with neuroendocrine carcinomas and 48 patients with well-differentiated tumors and/or metastases were included. The mean density of TAMs was 29, 43 and 234 CD68+ cells / 10 HPF in peritumoral exocrine pancreas, benign and malignant insulinomas, respectively (Figure 2B, P<0.001), indicating a significant correlation between increased macrophage infiltration and tumor progression (Figure 2A). The group of malignant insulinomas comprised 7 primary tumors, 5 infiltrated lymph nodes and 7 liver metastases. The highest infiltration of TAMs has been detected in liver metastases with a mean of 315 CD68+ cells / 10 HPF (P<0.05 compared to primary tumors and lymph nodes with 178 and 145 CD68+ cells, respectively). Moreover, the infiltration of CD68+ cells was significantly higher in malignant compared to benign insulinomas (43 vs. 178; P<0.01, Figure 2B). Similarly, poor differentiation defined as G3 neuroendocrine carcinomas (NEC) was associated to higher CD68+ macrophage infiltration compared to well-differentiated tumors (NEC vs. NET, 243 vs. 40 CD68+ cells, P<0.0001). The clinical correlation of these findings showed that in 6 out of 12 patients with NEC a disease-related death (DRD) occurred with a median overall survival of 27 months. In these patients, the CD68 score reached 303 positive cells on average. No DRD was documented in the group of patients with well-differentiated tumors.

TAMs in a genetically modified mouse model

To investigate a possible association between TAMs and PNET progression, we assessed TAM infiltration via F4/80 staining, the Ki-67 index and microvessel density via CD31 staining during the course of disease in the RIP1Tag2 transgenic mouse model. Representative slides for F4/80, Ki-67 and CD31 are shown in Supplemental Figure 1A. Sequential stages of hyperplastic (n = 17), angiogenic (n = 22) and invasive tumors (n = 18) demonstrated increased proliferation of tumor cells (mean Ki-67 values: 9%, 28% and 67%; Supplemental Figure 1C; P<0.001). The tumor stage-dependent proliferation was paralleled by a significantly increasing number of microvessels in hyperplastic (n = 16), angiogenic (n = 20) and invasive tumors (n = 20) (mean values CD31 positive cells / HPF: 11, 31 and 74; Supplemental Figure 1D; P<0.001). In analogy to these findings, infiltrating TAMs have been investigated in hyperplastic (n = 25), angiogenic (n = 12) and invasive tumors (n = 15): The mean numbers of F4/80+ cells / 10 HPF increased from 7 (hyperplastic) to 35 (angiogenic) and 85 (invasive tumors) (Supplemental Figure 1B; P<0.001), indicating an increasing infiltration of TAMs during the tumor progression.

Liposomal clodronate targets myeloid cells *in vitro* and *in vivo*

To elucidate the impact of therapeutic TAM modulation on tumor progression, liposomal clodronate has been used as an effective pharmacological tool to deplete macrophages in various *in vivo* models including a mouse model of pancreatic adenocarcinomas [29].

To evaluate the specificity of liposomal clodronate to target TAMs, we first investigated the susceptibility of several murine myeloid cell lines and human pancreatic neuroendocrine tumor cell lines to liposomal clodronate *in vitro*. To this extent, the myeloid cell lines J774, RAW and primary murine bone marrow-derived macrophages (mBMMs) from non-transgenic C57BL/6 mice as well as the neuroendocrine tumor cell lines Bon-1 and GQP1 were utilized. While no effect on cell viability was detected in the tumor cell lines, liposomal clodronate significantly affected cell viability of all investigated myeloid cells with a reduction of cell viability ranging between 39% and 87% after 24 hours (Figure 3).

In vivo studies to evaluate the impact of liposomal clodronate on PNET tumorigenesis and tumor progression were performed using the transgenic RIP1Tag2 model. Based on the multistage tumor progression in this model, we used two different

pharmacological intervention schemes with liposomal clodronate that allowed us to assess its effects both on the angiogenic switch during tumorigenesis ("prevention trial") and on the tumor progression ("intervention trial"). In the prevention trial, mice harbouring normal and hyperplastic islets were treated from week 6 to 13, while in the intervention trial mice were treated from week 9 to 16 (Figure 4A). Liposomal clodronate effectively decreased the number F4/80+ macrophages during tumor progression as shown in Supplemental Figure 2. In the prevention trial, liposomal clodronate reduced the cumulative tumor burden at week 13 significantly by 62% compared to PBS-liposomes (6.9×10^6 μm^2 vs. 2.6×10^6 μm^2; P=0.036, Table 2). While the number of hyperplastic, angiogenic and invasive islets remained unchanged in both groups, clodronate completely prevented the development of invasive tumors in 4 of 10 mice (P=0.025).

In the intervention trial, the influence of liposomal clodronate on tumor progression (number of invasive tumors: mean 4.6 vs. 2.2 per mice, P=0.069) and tumor volume (12.7×10^6 μm^2 vs. 10.2×10^6 μm^2, P=0.47) was less pronounced and did not reach statistical significance. Therefore, we speculated that TAMs are particularly important in early tumorigenesis during the progression from angiogenic to invasive islets. To further address this hypothesis, we assessed microvessel density (MVD) as cardinal feature of the angiogenic switch using CD31 immunhistochemistry as well as proliferation (Ki-67) and apoptosis marker (cleaved caspase-3). No differences between verum and placebo-treated animals were detected for Ki-67 and cleaved caspase-3 (Table 2). In contrast, CD31+ cells in invasive tumors were dramatically diminished in the intervention trial (39 vs. 22 positive cells per HPF, P=0.006) with a similar trend also in the prevention trial (77 vs. 48 positive cells per HPF, P=0.08). This indicates that angiogenesis is a critical step in mediating progression to invasive tumors, which is affected by macrophage depletion using liposomal clodronate. In order to characterize the depletion of F4/80+ cells more thoroughly, particularly effects on macrophage polarisation, we assessed arginase expression by immunohistochemistry as established marker for the protumoral M2 polariation of macrophages. Interestingly, no change was seen between liposomal clodronate and PBS-Liposomes treated mice, indicating that both M1 and M2 polarized macrophages are targeted by lipocomal clodronate.

Since depletion of F4/80+ macrophages may also affect T cell populations, we also stained the T cell marker CD3 and the marker for regulatory T cells FOXP3. In late

tumor stages clodronate application fostered the infiltration of CD3 positive cells (mean: 9 vs. 15 positive cells per HPF, P=0.034) in the intervention group. However, at earlier tumor stages this effect was not present and FOXP3 positive T cells were not regulated in both prevention and intervention cohorts (Table 2). Supplemental Figure 3 depicts representative stainings of Caspase 3, CD3, FOXP3 and Arginase in different tumor stages and lymphnodes.

Dual antiangiogenic therapy with sunitinib in combination with liposomal clodronate

Primary or acquired resistances frequently limit the efficacy of systemic antiangiogenic therapies such as sunitinib in PNET patients during the course of the disease. In preclinical models including the RIP1Tag2 mouse model previous reports proposed sunitinib-induced activation of escape mechanisms such as hypoxia, epithelial-mesenchymal transition (EMT), and other hypoxia-dependent signalling pathways [30-32] as mediators of resistance, thereby accelerating tumor aggressiveness and metastasis formation. Based on these data, we aimed to examine whether these escape mechanisms to antiangiogenic drugs can be overcome by targeting macrophages (Figure 4B).

First, we treated RIP1Tag2 mice with sunitinib monotherapy from week 12 to 16. Thereby, we could confirm that sunitinib resulted in remarkable reduction of microvessel density measured using an Anti-CD31 antibody (Table 3). However, no differences could be detected in terms of tumor number and volume (Table 3). In contrast to previous reports no liver metastases could be detected by H&E staining and immunohistochemistry using an SV40 antibody (data not shown). However, in the sunitinib group all mice (n=10) survived the treatment period, whereas two of ten mice in the placebo cohort died before sacrifice, potentially emphasizing a biochemical response during therapy via reducing insulin levels, although statistical significance was not reached due to small sample size.

Furthermore, we depleted macrophages via liposomal clodronate from week 9 to 16 and simultaneously administered sunitinib (from week 12 to 16). Combination treatment resulted in a significant reduction of both microvessel density (mean: 39 vs. 15 positive cells per HPF, P<0.001) and infiltrating TAMs (mean: 47 vs. 24 positive cells per HPF, P=0.003) (Table 3). However, no statistically significant synergies of dual antiangiogenic treatment regarding number of invasive islets or tumor volumes

compared to monotherapy could be detected. Likewise, no differences in proliferation and apoptosis markers or infiltrating CD3+, FOXP3+ or Arginase+ cells have been observed between combination and monotherapy strategies (Table 3). Similar to sunitinib monotherapy more mice reached the study endpoint of 16 weeks in the combination arm (9 vs. 6) compared to placebo therapy, however, this study has not been designed to evaluate overall survival.

Discussion

In this study, we utilized two independent cohorts of functional-active and non-functional active PNET tissue samples to investigate the infiltration of TAMs and its impact on tumor progression and metastasis. Our data clearly show that infiltrating TAMs are significantly correlated to tumor hallmarks such as angiogenesis, proliferation and metastasis. In addition, this study introduces liposomal clodronate as new therapeutic tool to target macrophages in pancreatic neuroendocrine tumors. Liposomal clodronate by depleting TAMs significantly impaired angiogenesis in the RipTag2 genetic mouse model of PNET. Our data suggest that pharmacological depletion of TAMs could serve as a suitable new therapeutic avenue for patients with unresectable disease. However, dual targeting of angiogenesis by simultaneous use of the clinically established multi-tyrosine kinase inhibitor sunitinib and liposomal clodronate in RIP1Tag2 mice failed to show synergistic anti-tumor or antiangiogenic efficacy.

Recently, TAMs were assessed in human PNETs samples with the degree of infiltration strongly correlating to proliferative activity, tumor grade and stage [19]. However, this study included only a small and heterogeneous patient cohort with 22 functional non-active (NF) and 5 functionally active (FA) PNETs without detailed characterization. TAM infiltration was only investigated in primary tumor samples. In our study, we used two independent cohorts of PNET including both primary tumors and metastases. In the first cohort, we could detect a remarkable difference between TAMs in primary tumors and distant metastases. However, this cohort also included heterogeneous tumor entities, both functionally active and non-active. Therefore, we aimed to confirm our data in a more homogeneous PNET cohort and used a TMA comprising benign and malignant insulinoma tissues including lymph node and liver metastases. Hereby, we could confirm the association between TAM infiltration, tumor progression and grading. In analogy to our findings, Wei and colleagues in

2014 reported a positive association between TAM infiltration and recurrence in a small cohort of 38 patients after curative resection of NF-PNETs [20]. In this report, TAM infiltration was only compared semiquantitatively. In contrast, in our series comprising more than 100 human samples TAM infiltration was quantified in absolute numbers per HPF which to our knowledge represents the largest study on TAMs in human PNET tissues.

In various cancer models TAMs have been shown to affect angiogenesis [33]. TAMs secrete a variety of proangiogenic growth factors, most prominently the vascular endothelial growth factor (VEGF), a cardinal mediator of tumor angiogenesis [34, 35]. TAM-induced upregulation of VEGF results in the so-called angiogenic switch that leads to enhanced microvessel formation and tumor progression. Our study clearly corroborate these findings showing a significantly reduced microvessel density following macrophage depletion.

Clodronate coated in liposomes has been widely used as experimental tool for macrophage depletion in several disease models including autoimmune disorders, atherosclerosis and cancer [36]. The use of liposomal clodronate has been reported in several xenograft tumor models [37, 38]. Recently, we depleted TAMs by liposomal clodronate in a mouse model of pancreatic adenocarcinoma (PDAC) [29]. Interestingly, in this model liposomal clodronate induced a significant decrease in metastasis formation. The size of the primary tumor, however, was only reduced to a minor extent [29]. We speculate that different angiogenic patterns in PDAC versus PNET might be responsible for this difference: PDAC primary tumors are largely hypovascular which limit the antiangiogenic effect of liposomal clodronate on the primary tumor. In these tumors, the effect of premetastatic niches in target organs liver and lung might be more important. In contrast, PNET tissues are highly vascularized resulting in an increased efficacy of antiangiogenic strategies in PNET tumors including therapeutic targeting of TAMs.

The depletory effect on macrophages appears to be a group effect and not to be restricted to liposomal-encapsulated clodronate. It has also been observed with other bisphosphonates such as zoledronate which has been shown to reduce viability of macrophages without affecting cancer cells *in vitro* and to diminish intratumoral macrophages in xenograft models *in vivo* [39, 40]. However, liposomal coating of drugs such as clodronate enhances their phagocytosis by cells such as macrophages, thereby increasing therapeutic efficacy. Generally, nanoparticle-coating of cytotoxic

drugs such as doxorubicin or irinotecan with liposomes is increasingly used to decrease toxicity and improve tolerability [41, 42]. However, human data on clodronate in neuroendocrine tumors are not available and the liposomal formulation has not been approved, yet. Thus, only conclusions from second-generation bisphosphonates can be drawn.

Despite of the pronounced effects of liposomal clodronate action on microvessel density and tumor progression, we failed to detect a significant synergism of liposomal clodronate with the antiangiogenic multikinase inhibitor sunitinib, which has been shown to target several VEGF-dependent signaling pathways *in vitro* and to significantly improve progression-free survival in PNET patients. This is in contrast to a report using xenograft HCC mouse models in which zoledronate was shown to overcome sunitinib- and sorafenib-induced IL12-dependent prometastatic resistance mechanisms [43]. The reasons for the lack of synergism in our *in vivo* model have yet to be elucidated. Previously, we have shown that liposomal clodronate leads to a pronounced downregulation of VEGF as main secretion product of TAM [29]. It may be speculated that both macrophage depletion and sunitinib application predominantly affect VEGF-dependent angiogenic pathways which could explain in part the lack of synergism in the highly VEGF-dependent PNET model.

Transgenic mouse models are an integral part of modern cancer research, however, the RIP1Tag2 model present some limitations in order to avoid general translation into the human system. From a biological point of view this model reflects higher proliferative tumors including NET G2 and G3 as well as poorly-differentiated carcinomas NEC G3 [21, 27]. Furthermore, the tumorigenesis in the RIP1Tag2 model does not include metastatic disease, although some groups demonstrated a metastatic spread upon treatment with targeted therapies [30]. In our hands, systematic evaluation of liver burden was excluded using SV40-T-antigen antibody. Regarding functionality, not all tumors can release insulin, however, all mice suffer from hypoglycemia as tumor-related cause of death. To this end, preclinical trials in this model must be designed to address pivotal challenges for higher proliferative pancreatic neuroendocrine tumors, whether functional active or not.

Taken together, our data indicate that TAM play a major role in tumor progression of pancreatic neuroendocrine tumors. Pharmacological macrophage depletion by liposomal clodronate leads to a pronounced antiangiogenic effect decreasing tumorigenesis and tumor progression, which could represent a new therapeutic

avenue for this highly angiogenic tumor entity. Based on our data, further studies are warranted to evaluate the role of bisphosphonates alone or in combination with established therapies such as somatostatin analogues or cytotoxic drugs in pancreatic neuroendocrine tumors.

Tables and Figures

Table 1:

Baseline characteristics of patients with non-metastatic NF-PNET primary tumors, insulinomas and metastatic NF-PNET.

Abbreviations: NF, non-functional active; PNET, pancreatic neuroendocrine tumor; G, grading; R, resection; M, metastases; SMS, somatostatin; SSA, somatostatin analogues

Table 1	NF-PNET N = 11		Insulinomas N = 21		Metastatic PNETs N = 13 Tissue of metastases N = 14 Tissue of primaries N = 4	
	value	%	value	%	value	%
Age at surgery (years)						
Median	54		48		58	
Range	30-79		18-72		31-73	
Tumor differentiation						
Well-differentiated	11	100%	21	100%	18	100%
Grading						
G1	9	82%	21	100%	1	8%
G2	2	18%	0		12	92%
R-Status						
R0	11	100%	19	90.5%		
R1	0	0%	2	9.5%		
M-Status						
M0	11	100%	11	100%	0	0%
M1	0	0%	0	0%	13	100%
Recurrence-free survival in months						
Median	44		9			
Range	5-133		3-15			
CD68 positive cells						
Average	170		163			
Range	13-367		31-809			
Sites of metastasis						

Liver						13	100%
LN						9	69%
SMS-Status							
Positive						12	92%
Surgical intervention							
Primary resection						9	69%
Metastatic surgery						9	69%
No surgery						3	23%
Medical treatment							
SSA						8	61.5%
Chemotherapy						13	100%
Chemoembolization						4	30.7%
CD68 positive cells							
Primaries						133	
Average						107-151	
Range							
Metastases						430	
Average						108-1251	
Range							

Table 2:

Results of the prevention and intervention trial in mice being treated with liposomal clodronate or PBS-Liposomes.

Abbreviations: SD, standard deviation

Table 2										
Features	Prevention Trial					Intervention Trial				
	PBS-Liposomes		Clodronate Liposomes			PBS-Liposomes		Clodronate Liposomes		
	mean	SD	mean	SD	P-value	mean	SD	mean	SD	P-value
Number of tumors	10.3	1.4	13.0	1.9	0.27	13.0	2.6	10.7	1.2	0.41
Number of invasive tumors	2.7	0.4	1.6	0.5	0.1	4.6	1.2	2.2	0.4	0.069
Prevalence of invasive tumors	**100%**		**60%**		**0.025**	100%		100%		1.0
Tumor area in µm²	**6.9 x10^6**	**1.8 x10^6**	**2.7 x10^6**	**0.9x 10^6**	**0.036**	12.7 x10^6	2.2 x10^6	10.2 x10^6	2.5x 10^6	0.47
Ki-67 index in invasive tumors	58%	3%	48%	6%	0.11	60%	3%	60	5%	0.99
CD31 positive	76.8	7.9	47.9	13.6	0.08	**39.2**	**2.2**	**22.1**	**3.9**	**0.006**

	mean	SD	mean	SD	P-value	mean	SD	mean	SD	P-value
cells per HPF										
Caspase 3 positive cells per HPF	10.6	1.3	10.6	2.4	0.99	22.1	6.7	15.5	2.7	0.36
CD3 positive cells per HPF	10.2	2.6	7.1	1.7	0.35	**9.3**	**2.2**	**15.2**	**1.2**	**0.034**
FOXP3 positive cells per HPF	3.1	1.1	3.1	0.7	0.97	4.4	0.4	10.1	2.7	0.091
Arginase positive cells per HPF	4.8	0.9	7.1	1.3	0.16	10.5	1.8	9.6	2.0	0.75

Table 3:

Results of the sunitinib monotherapy arm and the combination treatment of liposomal clodronat and sunitinib in an intervention setting.

Abbreviations: SD, standard deviation

Table 3										
Features	Sunitinib monotherapy					Combination Treatment				
	DMSO		Sunitinib			DMSO + PBS-Liposomes		Sunitinib + Clodronate Liposomes		
	mean	SD	mean	SD	P-value	mean	SD	mean	SD	P-value
Number of tumors	8.9	1.9	12.6	2.3	0.25	16.7	3.1	17.3	3.6	0.89
Number of invasive tumors	3.4	0.7	4.4	0.9	0.43	4.8	0.5	4.0	0.9	0.5
Prevalence of invasive tumors	100%		100%		1.0	100%		100%		1.0
Tumor area in μm^2	10.6×10^6	2.3×10^6	10.3×10^6	2.6×10^6	0.92	16.1×10^6	2.4×10^6	11.6×10^6	3.2×10^6	0.32
Ki-67 index in invasive tumors	70%	3%	65%	5%	0.42	72%	4%	77%	3%	0.32
CD31 positive	**33.1**	**2.9**	**16.3**	**2.4**	**0.004**	**39.2**	**2.7**	**14.6**	**2.7**	**0.001**

cells per HPF									
F4/80 positive cells per HPF	30.7	4.7	23.3	3.8	0.24	**43.9**	**4.2**	**23.4**	**1.7**	**0.003**
Caspase 3 positive cells per HPF	15.6	3.1	16.7	3.6	0.82	18.9	5.3	24.1	3.8	0.43
CD3 positive cells per HPF	19.5	3.3	14.1	1.8	0.14	22.8	4.5	19.6	3.5	0.59
FOXP3 positive cells per HPF	7.1	1.5	7.3	1.7	0.92	7.6	2.1	4.6	1.1	0.19
Arginase positive cells per HPF	5.4	1.4	4.2	0.9	0.49	**6.4**	**1.1**	**11.6**	**1.4**	**0.018**

Supplemental Table 1

Clinical and pathological features of patients with benign and malignant insulinomas.

Figure 1:

TAM infiltration correlates with malignant features of human PNETs. (A) Scheme of tissue included from patients with distinct functionality, stage and grading. Besides whole sections of paraffin blocks, a MTA carrying tissue of 83 insulinomas (including metastasis) was included. (B) Representative immunohistochemistry of CD68 positive cells in sections from PNETs and corresponding HE sections were shown with 40x original magnificantion. (C) Quantification of CD68 positive cells in whole paraffin sections (left) of 21 insulinomas, 11 non-metastatic NF-PNETs, 4 primaries of metastatic PNETs and 14 distant metastases. Data shown as mean ± SD. Symbols: dots represent data from each tissue; black horizontal line, mean percentage for each group.

Figure 2:

TAM infiltration in a MTA of human insulinomas. (A) 200-fold magnification of representative CD68 positive cells in normal pancreas, benign, malignant and metastasis. (B) Quantification of CD68 density in the insulinoma MTA (middle and

right). 19 normal pancreata were compared to 45 benign and 11 malignant insulinomas (middle). Fractions of malignant insulinomas with their sites of metastases were added at the right figure with 7 primary malignant insulinomas, 5 lymph node and 7 liver metastases. Data shown as mean ± SD. Symbols: dots represent data from each tissue; black horizontal line, mean percentage for each group.

Figure 3:

Liposomal clodronate decelerated tumor progression *in-vitro* and *in-vivo*. (A) Human pancreatic neuroendocrine tumor cell lines Bon-1 and QGP1 were treated with PBS-Liposomes, 0.1mg and 1mg liposomal clodronate for 24h. Similarly, the myeloid cell lines J774, RAW and murine bone marrow-derived macrophages (mBMM) from non-transgenic mice were treated uniquely. Assays were performed in triplicate and cell viability was determined by ATP-based assay. Data are presented as mean ± SD and are representative of three independent experiments.

Figure 4:

(A) Treatment scheme of the prevention (week 6-13) and intervention (week 9-16) trial. Liposomal clodronate or PBS-Liposomes were applied intraperitoneal in RIP1Tag2 mice biweekly. (B) Treatment scheme of sunitnib monotherapy (week 12-16) daily given per os and the combination of sunitinib and liposomal clodronate (week 9-16), which was administered biweekly intraperitoneal compared to DMSO and PBS-Liposomes as control arm.

Supplemental Figure 1:

TAM infiltration correlates with proliferation and angiogenesis during tumor progression in the RIP1Tag2 model. (A) Representative immunohistochemistry of HE, F4/80, Ki-67 and CD31 positive cells in distinct stages of the RIP1Tag2 tumorigenesis including hyperplastic, angiogenic and invasive tumors. 40x original magnicantion is presented. (B) F4/80 positive cells per HPF were counted in 25 hyperplastic, 12 angiogenic and 15 invasive islets. (C) Ki-67 index in % was measured in 17 hyperplastic, 22 angiogenic and 18 invasive islets. (D) CD31 positive cells per HPF were counted in 16 hyperplastic, 20 angiogenic and 20 invasive

tumors. Data shown as mean ± SD. Symbols: dots represent data from each islet; black horizontal line, mean percentage for each group.

Supplemental Figure 2:

TAM infiltration decreases upon liposomal clodronate therapy. All macrophages were counted and afterwards normalized to all islets in the tumor. Median TAM infiltration normalized to all islets was 22 +/- 3.7 SD in the PBS-Liposomes group compared to 12 +/- 2.2 in the clodronate arm for the prevention trial (P=0.044). 65 +/- 6.7 SD (PBS-Liposomes) and 22 +/- 4.7 (clodronate) were the results for the intervention group, respectively (P=0.0007)).

Supplemental Figure 3:

Representative immunohistochemistry of Caspase 3, CD3, FOXP3 and Arginase positive cells in distinct stages of the RIP1Tag2 tumorigenesis including hyperplastic, angiogenic and invasive tumors. 40x original magnificantion is presented. Positive cells were counted in at least 10 HPF. Positive cells in lymph nodes served as internal control.

References

1. Hanahan D, Weinberg RA. Hallmarks of cancer: the next generation. *Cell* 2011;**144**: 646-74.

2. Hanahan D, Coussens LM. Accessories to the crime: functions of cells recruited to the tumor microenvironment. *Cancer Cell* 2012;**21**: 309-22.

3. Quail DF, Joyce JA. Microenvironmental regulation of tumor progression and metastasis. *Nat Med* 2013;**19**: 1423-37.

4. Steidl C, Lee T, Shah SP, Farinha P, Han G, Nayar T, Delaney A, Jones SJ, Iqbal J, Weisenburger DD, Bast MA, Rosenwald A, et al. Tumor-associated macrophages and survival in classic Hodgkin's lymphoma. *N Engl J Med* 2010;**362**: 875-85.

5. Robinson BD, Sica GL, Liu YF, Rohan TE, Gertler FB, Condeelis JS, Jones JG. Tumor microenvironment of metastasis in human breast carcinoma: a potential prognostic marker linked to hematogenous dissemination. *Clin Cancer Res* 2009;**15**: 2433-41.

6. Hussain SF, Yang D, Suki D, Aldape K, Grimm E, Heimberger AB. The role of human glioma-infiltrating microglia/macrophages in mediating antitumor immune responses. *Neuro Oncol* 2006;**8**: 261-79.

7. Di Caro G, Cortese N, Castino GF, Grizzi F, Gavazzi F, Ridolfi C, Capretti G, Mineri R, Todoric J, Zerbi A, Allavena P, Mantovani A, et al. Dual prognostic significance of tumour-associated macrophages in human pancreatic adenocarcinoma treated or untreated with chemotherapy. *Gut* 2016;**65**: 1710-20.

8. Shree T, Olson OC, Elie BT, Kester JC, Garfall AL, Simpson K, Bell-McGuinn KM, Zabor EC, Brogi E, Joyce JA. Macrophages and cathepsin proteases blunt chemotherapeutic response in breast cancer. *Genes Dev* 2011;**25**: 2465-79.

9. Gocheva V, Wang HW, Gadea BB, Shree T, Hunter KE, Garfall AL, Berman T, Joyce JA. IL-4 induces cathepsin protease activity in tumor-associated macrophages to promote cancer growth and invasion. *Genes Dev* 2010;**24**: 241-55.

10. Mitchem JB, Brennan DJ, Knolhoff BL, Belt BA, Zhu Y, Sanford DE, Belaygorod L, Carpenter D, Collins L, Piwnica-Worms D, Hewitt S, Udupi GM, et al. Targeting tumor-infiltrating macrophages decreases tumor-initiating cells, relieves immunosuppression, and improves chemotherapeutic responses. *Cancer Res* 2013;**73**: 1128-41.

11. Mosser DM, Edwards JP. Exploring the full spectrum of macrophage activation. *Nat Rev Immunol* 2008;**8**: 958-69.

12. Biswas SK, Mantovani A. Macrophage plasticity and interaction with lymphocyte subsets: cancer as a paradigm. *Nat Immunol* 2010;**11**: 889-96.

13. Halfdanarson TR, Rabe KG, Rubin J, Petersen GM. Pancreatic neuroendocrine tumors (PNETs): incidence, prognosis and recent trend toward improved survival. *Ann Oncol* 2008;**19**: 1727-33.

14. Panzuto F, Boninsegna L, Fazio N, Campana D, Pia Brizzi M, Capurso G, Scarpa A, De Braud F, Dogliotti L, Tomassetti P, Delle Fave G, Falconi M. Metastatic and locally advanced pancreatic endocrine carcinomas: analysis of factors associated with disease progression. *J Clin Oncol* 2011;**29**: 2372-7.

15. Rindi G, Falconi M, Klersy C, Albarello L, Boninsegna L, Buchler MW, Capella C, Caplin M, Couvelard A, Doglioni C, Delle Fave G, Fischer L, et al. TNM staging of neoplasms of the endocrine pancreas: results from a large international cohort study. *J Natl Cancer Inst* 2012;**104**: 764-77.

16. Pape UF, Berndt U, Müller-Nordhorn J, Böhmig M, Roll S, Koch M, Willich SN, Wiedenmann B. Prognostic factors of long-term outcome in gastroenteropancreatic neuroendocrine tumours. *Endocr Relat Cancer* 2008;**15**: 1083-97.

17. Jiao Y, Shi C, Edil BH, de Wilde RF, Klimstra DS, Maitra A, Schulick RD, Tang LH, Wolfgang CL, Choti MA, Velculescu VE, Diaz LA, et al. DAXX/ATRX, MEN1, and mTOR pathway genes are frequently altered in pancreatic neuroendocrine tumors. *Science* 2011;**331**: 1199-203.

18. Scarpa A, Chang DK, Nones K, Corbo V, Patch AM, Bailey P, Lawlor RT, Johns AL, Miller DK, Mafficini A, Rusev B, Scardoni M, et al. Whole-genome landscape of pancreatic neuroendocrine tumours. *Nature* 2017;**543**: 65-71.

19. Pyonteck SM, Gadea BB, Wang HW, Gocheva V, Hunter KE, Tang LH, Joyce JA. Deficiency of the macrophage growth factor CSF-1 disrupts pancreatic neuroendocrine tumor development. *Oncogene* 2012;**31**: 1459-67.

20. Wei IH, Harmon CM, Arcerito M, Cheng DF, Minter RM, Simeone DM. Tumor-associated macrophages are a useful biomarker to predict recurrence after surgical resection of nonfunctional pancreatic neuroendocrine tumors. *Ann Surg* 2014;**260**: 1088-94.

21. Hanahan D. Heritable formation of pancreatic beta-cell tumours in transgenic mice expressing recombinant insulin/simian virus 40 oncogenes. *Nature* 1985;**315**: 115-22.

22. Gocheva V, Chen X, Peters C, Reinheckel T, Joyce JA. Deletion of cathepsin H perturbs angiogenic switching, vascularization and growth of tumors in a mouse model of pancreatic islet cell cancer. *Biol Chem* 2010;**391**: 937-45.

23. Hunter KE, Palermo C, Kester JC, Simpson K, Li JP, Tang LH, Klimstra DS, Vlodavsky I, Joyce JA. Heparanase promotes lymphangiogenesis and tumor invasion in pancreatic neuroendocrine tumors. *Oncogene* 2014;**33**: 1799-808.

24. Akkari L, Gocheva V, Quick ML, Kester JC, Spencer AK, Garfall AL, Bowman RL, Joyce JA. Combined deletion of cathepsin protease family members reveals compensatory mechanisms in cancer. *Genes Dev* 2016;**30**: 220-32.

25. Parekh D, Ishizuka J, Townsend CM, Haber B, Beauchamp RD, Karp G, Kim SW, Rajaraman S, Greeley G, Thompson JC. Characterization of a human pancreatic carcinoid in vitro: morphology, amine and peptide storage, and secretion. *Pancreas* 1994;**9**: 83-90.

26. Casanovas O, Hicklin DJ, Bergers G, Hanahan D. Drug resistance by evasion of antiangiogenic targeting of VEGF signaling in late-stage pancreatic islet tumors. *Cancer Cell* 2005;**8**: 299-309.

27. Hanahan D, Folkman J. Patterns and emerging mechanisms of the angiogenic switch during tumorigenesis. *Cell* 1996;**86**: 353-64.

28. Kaplan E. Nonparametric estimation from incomplete observations. In: Meier P, ed., vol. 53 Journal of the American Statistical Association, 1958:281-4.

29. Griesmann H, Drexel C, Milosevic N, Sipos B, Rosendahl J, Gress TM, Michl P. Pharmacological macrophage inhibition decreases metastasis formation in a genetic model of pancreatic cancer. *Gut* 2016.

30. Maione F, Capano S, Regano D, Zentilin L, Giacca M, Casanovas O, Bussolino F, Serini G, Giraudo E. Semaphorin 3A overcomes cancer hypoxia and metastatic dissemination induced by antiangiogenic treatment in mice. *J Clin Invest* 2012;**122**: 1832-48.

31. Bergers G, Javaherian K, Lo KM, Folkman J, Hanahan D. Effects of angiogenesis inhibitors on multistage carcinogenesis in mice. *Science* 1999;**284**: 808-12.

32. Pàez-Ribes M, Allen E, Hudock J, Takeda T, Okuyama H, Viñals F, Inoue M, Bergers G, Hanahan D, Casanovas O. Antiangiogenic therapy elicits malignant progression of tumors to increased local invasion and distant metastasis. *Cancer Cell* 2009;**15**: 220-31.

33. Noy R, Pollard JW. Tumor-associated macrophages: from mechanisms to therapy. *Immunity* 2014;**41**: 49-61.

34. Kujawski M, Kortylewski M, Lee H, Herrmann A, Kay H, Yu H. Stat3 mediates myeloid cell-dependent tumor angiogenesis in mice. *The Journal of clinical investigation* 2008;**118**: 3367-77.

35. Sun B, Karin M. The therapeutic value of targeting inflammation in gastrointestinal cancers. *Trends in pharmacological sciences* 2014;**35**: 349-57.

36. van Rooijen N, van Kesteren-Hendrikx E. Clodronate liposomes: perspectives in research and therapeutics. *J Liposome Res* 2002;**12**: 81-94.

37. Zeisberger SM, Odermatt B, Marty C, Zehnder-Fjällman AH, Ballmer-Hofer K, Schwendener RA. Clodronate-liposome-mediated depletion of tumour-associated macrophages: a new and highly effective antiangiogenic therapy approach. *Br J Cancer* 2006;**95**: 272-81.

38. Reusser NM, Dalton HJ, Pradeep S, Gonzalez-Villasana V, Jennings NB, Vasquez HG, Wen Y, Rupaimoole R, Nagaraja AS, Gharpure K, Miyake T, Huang J, et al. Clodronate inhibits tumor angiogenesis in mouse models of ovarian cancer. *Cancer Biol Ther* 2014;**15**: 1061-7.

39. Rietkötter E, Menck K, Bleckmann A, Farhat K, Schaffrinski M, Schulz M, Hanisch UK, Binder C, Pukrop T. Zoledronic acid inhibits macrophage/microglia-assisted breast cancer cell invasion. *Oncotarget* 2013;**4**: 1449-60.

40. Rogers TL, Wind N, Hughes R, Nutter F, Brown HK, Vasiliadou I, Ottewell PD, Holen I. Macrophages as potential targets for zoledronic acid outside the skeleton-evidence from in vitro and in vivo models. *Cell Oncol (Dordr)* 2013;**36**: 505-14.

41. Slingerland M, Guchelaar HJ, Gelderblom H. Liposomal drug formulations in cancer therapy: 15 years along the road. *Drug Discov Today* 2012;**17**: 160-6.

42. Wang-Gillam A, Li CP, Bodoky G, Dean A, Shan YS, Jameson G, Macarulla T, Lee KH, Cunningham D, Blanc JF, Hubner RA, Chiu CF, et al. Nanoliposomal irinotecan with fluorouracil and folinic acid in metastatic pancreatic cancer after previous gemcitabine-based therapy (NAPOLI-1): a global, randomised, open-label, phase 3 trial. *Lancet* 2016;**387**: 545-57.

43. Zhang W, Zhu XD, Sun HC, Xiong YQ, Zhuang PY, Xu HX, Kong LQ, Wang L, Wu WZ, Tang ZY. Depletion of tumor-associated macrophages enhances the effect of sorafenib in metastatic liver cancer models by antimetastatic and antiangiogenic effects. *Clin Cancer Res* 2010;**16**: 3420-30.
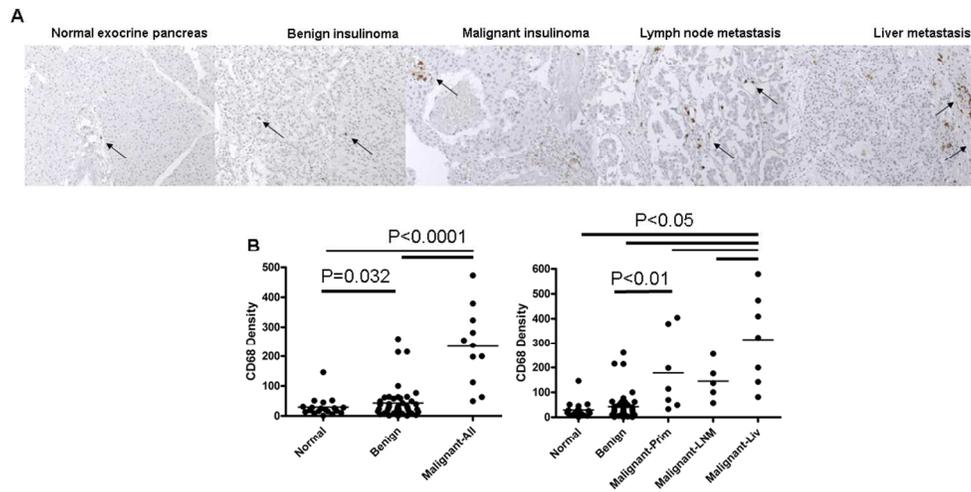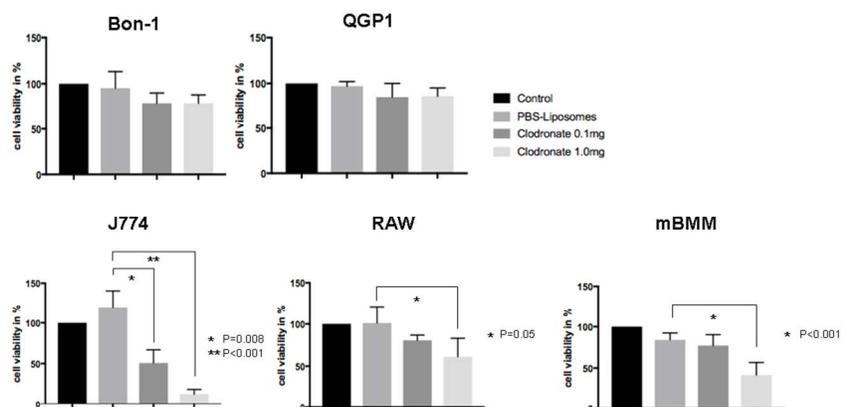
Figure 1
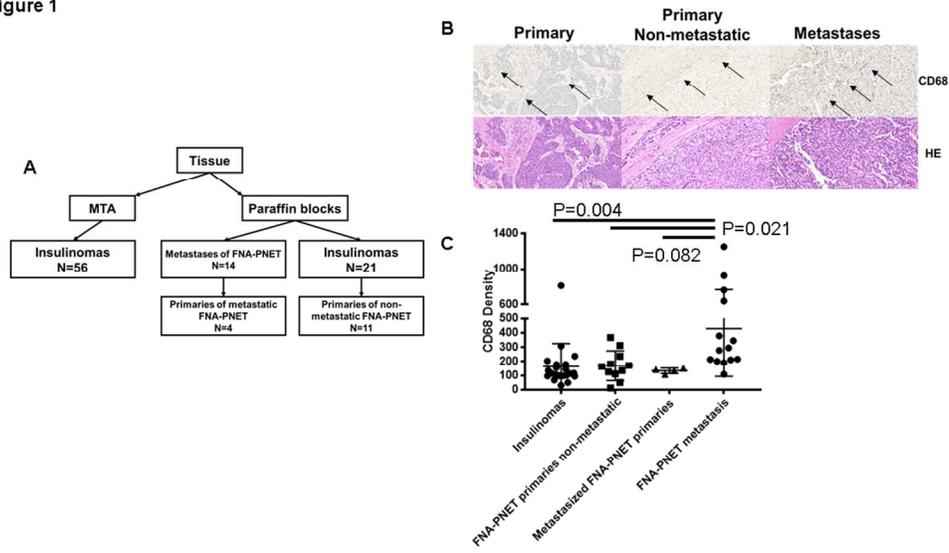
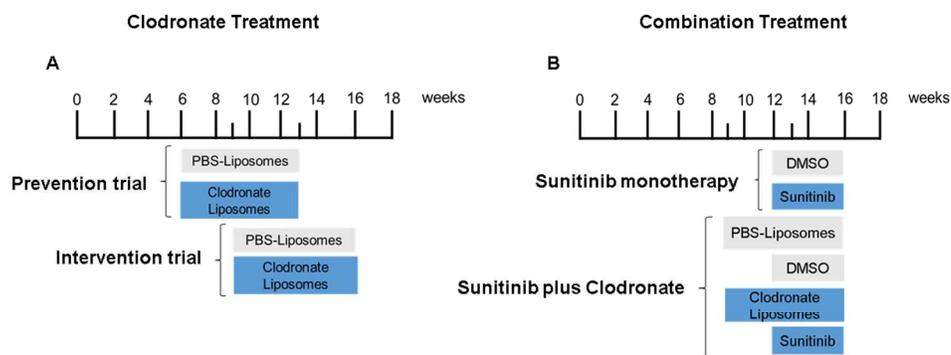338x190mm (96 x 96 DPI)

Figure 2

338x190mm (96 x 96 DPI)

Figure 3

338x190mm (96 x 96 DPI)

Figure 4

338x190mm (96 x 96 DPI)